IET Electric Power Applications

Research Article

IET Journals
The Institution of Engineering and Technology

Rotor fault diagnosis in permanent magnet synchronous machine using the midpoint voltage of windings

ISSN 1751-8660
Received on 10th June 2019
Revised 27th September 2019
Accepted on 25th October 2019
E-First on 16th January 2020
doi: 10.1049/iet-epa.2019.0428
www.ietdl.org

José Bossio[1] ✉, Cristian Ruschetti[2], Guillermo Bossio[1], Carlos Verucchi[2], Cristian De Angelo[1]

[1]*IITEMA-CONICET, GEA-UNRC, Ruta Nac. #36, km 601, Río Cuarto, Córdoba, Argentina*
[2]*INTELYMEC-UNCPBA, CIFICEN-CICPBA-CONICET, Del Valle 5737, Olavarría, Argentina*
✉ *E-mail: jbossio@ing.unrc.edu.ar*

Abstract: A new strategy is proposed here for the diagnosis of asymmetric demagnetisation in permanent magnet synchronous machines. The strategy is based on the measuring of the voltage at the midpoint of the windings within a phase. Unlike the phase voltage, for a fault situation, the midpoint voltage shows sidebands around the fundamental component, which allows detecting and quantifying the demagnetisation phenomenon. A low-cost implementation for the automatic detection of faults is also proposed in the present study and experimental results are presented to validate the strategy.

1 Introduction

The use of permanent magnet synchronous machines (PMSMs) has increased significantly, mainly due to improvements in the development of alloys of magnetic materials used in the construction of permanent magnets [1, 2]. PMSMs are widely used in applications such as electric motor drives and generators for renewable energy plants. The main advantages of the PMSMs over induction machines are those associated with high power density and high performance [1, 3]. This fact, together with the global trend in the efficient use of energy, makes them an interesting alternative for many applications.

Faults originated in the PMSMs can be classified as: stator faults, rotor faults and bearing faults [4]. Regarding the stator faults, they are mainly caused by short circuits between winding coils [5–8] as well as those in the stator core. In the case of rotor faults, they are commonly due to eccentricity [9] or rotor demagnetisation [10–12]. These faults are related to high costs, not only due to the repair of the PMSM but also by the unscheduled downtime of the equipment where the machine is located.

Usually, the rotor demagnetisation in the PMSM can be caused by the presence of thermal, mechanical or electrical stresses, as well as due to environmental conditions [13]. Demagnetisation of magnets produces a reduction in the electromotive force (EMF) induced in the stator windings. Therefore, if the PMSM is requested to produce the same output power than in the healthy machine condition, the currents in the stator windings are increased [13, 14]. This increase of currents above their nominal values produces a temperature rise in the windings and therefore in the machine, which can contribute to demagnetisation of magnets increasing indeed the fault severity.

There are several proposals to detect faults in PMSMs. A recent review of the current state of the art of condition monitoring and fault diagnosis techniques for PMSM is presented in [15]. In [16] a strategy for the detection and separation of rotor problems in PMSMs such as eccentricity and oscillation in the load torque is proposed. The harmonic frequencies induced in the EMF due to demagnetisation faults are analysed in [11] and a method for detection based on the zero-sequence voltage is proposed.

The detection of rotor faults in PMSMs under non-stationary operating conditions using time–frequency methods and spectral analysis is reported in [4]. For this particular case, two methods are applied that use the windowed Fourier transform and Wigner–Ville distributions for detecting frequencies associated with rotor failures.

On the other hand, in [17] a review of demagnetisation fault diagnosis methods in PMSM is presented. For the development of detection and diagnosis strategies, models that include the effects of faults are needed. This allows for evaluating different possible scenarios without the necessity of an experimental prototype. The effects of the demagnetisation in a four-pole PMSM with series and parallel windings are analysed in [18] using the finite element method (FEM). The results showed that the behaviour of the PMSM under demagnetisation changes significantly for different connections of stator windings. A characterisation of faults due to demagnetisation for different winding distributions using FEM simulations is presented in [19]. A model for the analysis of partial demagnetisation of the PMSM rotor is presented in [10]. In the same way in [20], through FEM simulations and experimental results, a simple dynamic *abc* model for brushless permanent magnet motors, under demagnetisation faults, is presented and validated.

The strategies based on the analysis of the harmonics produced by rotor demagnetisation in the phase currents or the EMF are very dependent on the distribution and connection of the windings [17–19]. Additionally, other problems such as motor asymmetries, unbalance or distorted voltages, and load imbalance can produce the same components in the EMF or phase currents, thus making the diagnosis more difficult. To avoid these inconveniences, the use of search coils for fault diagnosis in PMSM is proposed in [21]. Although the technique is invasive, it is suitable for critical applications, where it is also necessary to have the capability of evaluating the severity and the location of each fault. This need is because an unexpected fault of the machine could lead to a very high repair or replacement cost, or even the catastrophic system failure, such as is in the case of the aerospace industry, automotive industry or wind turbines, among others applications.

A new strategy for fault diagnosis due to asymmetric demagnetisation in PMSMs is proposed and developed in this paper. The strategy is based on the measuring of the voltage at the midpoint of the windings within a phase. In Section 2, an analytical model to evaluate demagnetisation effects on the EMF induced in the whole winding and a half winding is developed. It analyses the condition of the machine under both no-fault and fault conditions. A diagnosis strategy based on the evaluation of the sidebands arising after a fault in the voltage at the midpoint of the windings of a phase is also proposed in this section. Through the midpoint voltage analysis, a fault severity factor is proposed, given by the relation between the mentioned sidebands and the fundamental component. The diagnosis strategy is validated in Section 3 using the experimental results obtained from a laboratory prototype.

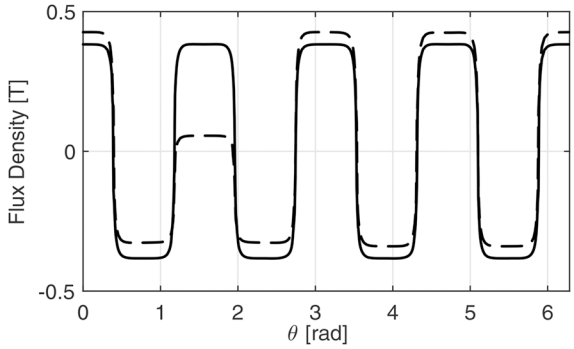

Fig. 1 *Flux density for a PMSM with P = 4. Healthy (solid line) and with total demagnetisation in one pole, $\mu = 1$ (dashed line)*

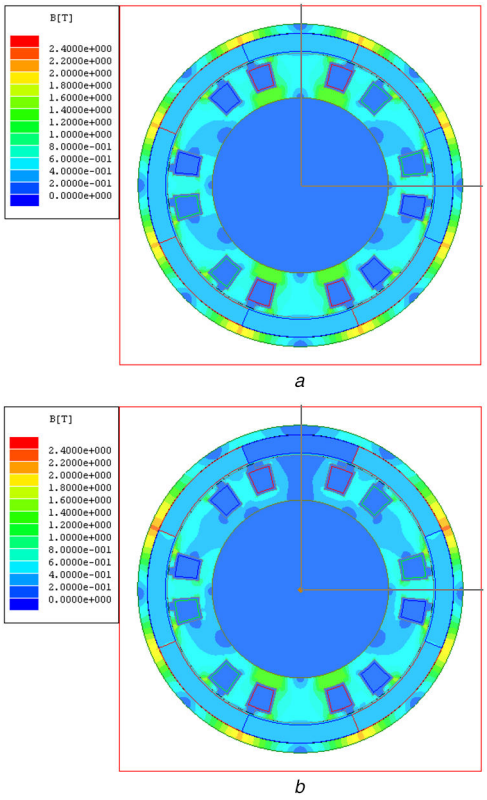

Fig. 2 *Flux density of a PMSM with P = 4*
(a) Healthy, ***(b)*** Total demagnetisation in one pole

From these results, simple implementation for demagnetisation fault detection using the voltages measured at the midpoint of the winding is proposed in Section 4. Finally, conclusions are given in Section 5.

2 EMF analysis

In order to evaluate the effects produced by asymmetric demagnetisation, an analysis of the changes generated by this fault in the components of the total phase EMF and the partial EMF of the windings is proposed. From this analysis, the characteristic components of the spectrum to be used for fault diagnosis are determined.

The EMF induced in any stator winding, $e(t)$, can be obtained from the derivative of the linked flux ψ_s [20]:

$$e(t) = -\frac{\mathrm{d}\psi_s}{\mathrm{d}t} = -\frac{\mathrm{d}\psi_s}{\mathrm{d}\theta_r}\frac{\mathrm{d}\theta_s}{\mathrm{d}t} = \varphi(\theta_r)\omega_r \tag{1}$$

where θ_r and ω_r are the rotor position and angular speed, respectively.

The flux linked by the stator circuits is obtained by integrating the flux density B over the region occupied by the windings. Assuming the radial flux density and the coils along the axial axis of the machine are uniform, the flux linked by a stator winding is given by

$$\psi_s(\theta_r) = rl\int_0^{2\pi} N(\theta_s)B(\theta_s - \theta_r)\,\mathrm{d}\theta_s \tag{2}$$

where r is the mean radius of the air gap, l is the axial length of the core and N is winding distribution as a function of a reference angle θ_s.

2.1 EMF of the healthy PMSM

For a PMSM with symmetrical winding and P pairs of poles, the winding distribution function for a given phase is

$$N_s(\theta_s) = \sum_{\substack{n=1\\ n\ \text{odd}}}^{\infty} N_n\cos(nP\theta_s) \tag{3}$$

Moreover, for no fault in the rotor, the flux density can be written as

$$B(\theta_s\theta_r) = \sum_{\substack{n=1\\ n\ \text{odd}}}^{\infty} B_n\cos(nP(\theta_s - \theta_r)) \tag{4}$$

In (3) and (4), N and B are periodic functions in the interval $[0, 2\pi/P]$. Thus, by replacing (3) and (4) into (2), an integral of a sum of sine and cosine can be obtained. In this integral, the only terms that cannot be cancelled are those with the same argument, resulting

$$\psi_s(\theta_r) = \pi rl\sum_{\substack{n=1\\ n\ \text{odd}}}^{\infty} N_nB_n\cos(nP\theta_r) \tag{5}$$

Then, the EMF is obtained by taking the time derivative of the linked flux (5). Considering that the rotor speed is constant, $\theta_r = \omega_r t$, then the EMF is defined as follows:

$$e(t) = K\omega_s\sum_{\substack{n=1\\ n\ \text{odd}}}^{\infty} nN_nB_n\sin(n\omega_s t) \tag{6}$$

where $K = \pi rl/P$ and $\omega_s = P\omega_r$. From this expression it can be observed that the components that appear in the EMF are those present in both, the winding distribution and the rotor flux distribution. For the case with N_n or B_n equal to zero, the corresponding component will not appear in the EMF of the PMSM phase. Expression (6) also shows that only the fundamental frequency component, $f_s = \omega_s/2\pi$, and its harmonics $f_{sn} = nf_s$ appear in the EMF.

2.2 EMF of the PMSM with fault

Considering the asymmetric rotor demagnetisation, the flux is asymmetric between each pair of poles and is only periodic within the interval $[0, 2\pi]$. As an example, Fig. 1 shows the flux density distributions, obtained by the FEM, for a PMSM with four pairs of poles, no fault and total demagnetisation on one pole. Similar effects can also be seen in the machine structure calculated by the FEM (Fig. 2) on the distribution of flux density. In consequence, the flux can be written as follows:

$$B_f(\theta_s, \theta_r) = \sum_{m=1}^{\infty} B_m^f\cos(m(\theta_s, \theta_r)) \tag{7}$$

The original components of flux, whose amplitudes reduce as a function of demagnetisation, can be obtained in (7), when $m = nP$

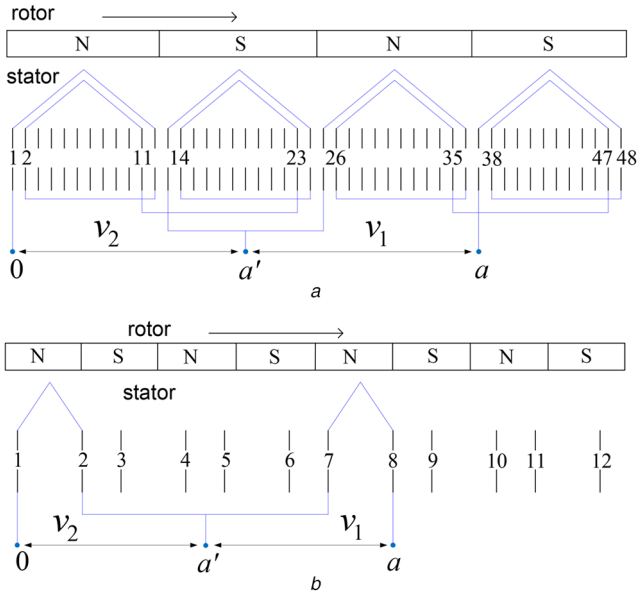

Fig. 3 *PMSM winding distributions and midpoint connection*
(a) Distributed windings with $P = 2$, ***(b)*** Concentrated windings with $P = 4$

with $n = 1, 3, 5, \ldots$. Moreover, new components appear for $m \neq nP$ whose amplitudes depend on the severity of the fault.

We define the fault severity, μ, as the percentage of demagnetisation on one rotor pole, so that $\mu = 0$ corresponds to a completely healthy pole and $\mu = 1$ a demagnetised pole. From this definition, it is possible to approximate the value of each flux component, as proposed in [10]. Thus, from (7), if $m = nP$, the flux density distribution components, B_n, change their amplitudes as functions of μ according to [10]:

$$B_m^{\mathrm{f}} \simeq B_n\left(1 - \frac{u}{2P}\right) \tag{8}$$

That is the amplitudes of both the fundamental component and the flux density harmonics decrease similarly compared with values for no demagnetisation. Moreover, as the number of pairs of poles increases, the effects on these components of demagnetisation in a single pole piece decrease.

On the contrary, as proposed in [10], if $m \neq nP$, then

$$B_m^{\mathrm{f}} \simeq \frac{2}{\pi} B_{\mathrm{M}} \frac{\mu}{m} \sin\left(\frac{m\pi}{2P}\right) \tag{9}$$

where B_{M} is the maximum value of the flux density.

These new components of flux density due to the asymmetry and their amplitudes vary linearly with the demagnetisation. Equations (8) and (9) are consistent with those obtained in [11] for the amplitude of the EMF voltage components in one slot. Note that if the PMSM has only one pair of poles ($P = 1$), no new components in the flux density due to demagnetisation appear and only a decrease of the original components is manifested, conserving the same distribution.

Using (3) and (7), the EMF induced in a phase-winding results in

$$e(t) = K\omega_{\mathrm{s}} \sum_{\substack{n=1 \\ n\,\mathrm{odd}}}^{\infty} nN_n B_{nP}^{\mathrm{f}} \sin(n\omega_{\mathrm{s}} t) \tag{10}$$

From this equation, it can be concluded that for a fault at the magnets, a variation in the flux distribution changes the amplitude of the fundamental component and that of the harmonics of the induced EMF but it produces no new components in the EMF. Therefore, no new components appear in the current or torque due to fault neither that allow diagnosis. A similar conclusion is obtained in [11, 14] using a similar approach for PMSM with windings symmetrically distributed and connected in series.

2.3 EMF in the windings

Unlike the distribution of the whole winding of one phase, the distribution of a single coil or group of coils of one phase is periodic only in the interval $[0, 2\pi]$. For this reason, the new components that appear in the flux density due to fault (9) can induce new characteristic components in the EMF.

In this work, in order to measure these components on the EMF, it is proposed to allow access to the midpoint of a winding phase. Thus, the distribution of each two circuits of the stator phase (N_{s1} and N_{s2}) is periodic in the range $[0, 2\pi]$ and is given by [14]

$$N_{s1}(\theta_{\mathrm{s}}) = \sum_{\substack{n=1 \\ n\,\mathrm{odd}}}^{\infty} \left(N_n^1 \cos(n\,P\,\theta_{\mathrm{s}}) + H_n^1 \cos(n\,\theta_{\mathrm{s}})\right) \tag{11}$$

$$N_{s2}(\theta_{\mathrm{s}}) = \sum_{\substack{n=1 \\ n\,\mathrm{odd}}}^{\infty} \left(N_n^1 \cos(n\,P\,\theta_{\mathrm{s}}) - H_n^1 \cos(n\,\theta_{\mathrm{s}})\right) \tag{12}$$

In these equations, it can be seen that the distribution of the second circuit is obtained by displacing π (rad) from the first one:

$$N_{s2}(\theta_{\mathrm{s}}) = N_{s1}(\theta_{\mathrm{s}} + \pi) \tag{13}$$

If the two distributions shown in (11) and (12) are added to form the complete winding distribution of the phase, all odd terms are cancelled resulting in the equation presented in (3) with $N_n = 2N_n^1$.

By calculating the EMF for each circuit, as it was calculated for the whole winding of the phase yields:

$$e_1(t) = \sum_{\substack{n=1 \\ n\,\mathrm{odd}}}^{\infty} \left(C_n \sin(n\omega_{\mathrm{s}} t) + D_n \sin\left(\frac{n\omega_{\mathrm{s}}}{P} t\right)\right) \tag{14}$$

$$e_2(t) = \sum_{\substack{n=1 \\ n\,\mathrm{odd}}}^{\infty} \left(C_n \sin(n\omega_{\mathrm{s}} t) - D_n \sin\left(\frac{n\omega_{\mathrm{s}}}{P} t\right)\right) \tag{15}$$

where

$$C_n = \omega_{\mathrm{s}} K n N_n^1 B_{nP}^f \tag{16}$$

$$D_n = \omega_{\mathrm{s}} K n N_n^1 B_n^f \tag{17}$$

Like for the complete winding of the phase, the amplitude of each harmonic C_n decreases due to demagnetisation. However, new components of amplitude D_n appear on each circuit, defined by

$$f_n = \frac{n}{P} f_{\mathrm{s}} \quad \text{with } n \text{ odd}\,. \tag{18}$$

These components are in counterphase for the two circuits. Therefore, if the circuits are connected in series, then the components become null obtaining the same result as in (10).

2.4 Detection of the fault and severity factor

According to what was developed in the previous section, it is possible to detect the asymmetric demagnetisation by analysing the EMF components given by (18) that appear in the middle point of the phase winding as a result of the fault.

For that a connection of the midpoint of a phase winding is necessary. This connection is not available in many commercial motors but it is very easy to implement during the manufacturing or rewinding process. As an example, Fig. 3 shows the midpoint connection for two different motors. The first scheme corresponds to a stator with distributed windings and $P = 2$, and the second one corresponds to a stator with concentrated windings and $P = 4$. In these schemes, only the phase 'a' winding is shown.

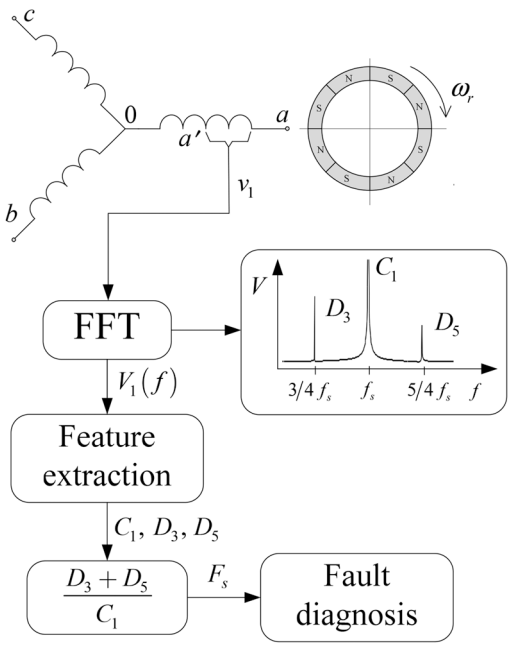

Fig. 4 *Fault diagnosis strategy*

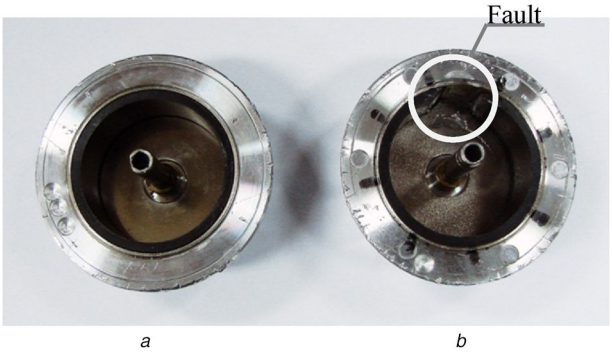

Fig. 5 *Rotors of the PMSM*
(a) Healthy, ***(b)*** With fault

From the EMF spectrum, the components with the highest amplitude produced by the asymmetric demagnetisation are the closest to the fundamental frequency f_s. Thus, for motors with $P = 2$, the most significant components are the ones with $n = 1$ and $n = 3$. However, for $P = 4$, these components are with $n = 3$ and $n = 5$. In the latter case, the amplitude of these components at frequencies $3/4f_s$ and $5/4f_s$, correspond to D_3 and D_5, respectively.

To estimate the fault severity, it is necessary to define a severity factor F_s using the characteristic components due to fault. This severity factor should be insensitive to variations at the operating point of the machine.

In this paper, we propose the fault severity factor for a machine with $P = 4$:

$$F_s = \left(\frac{D_3 + D_5}{C_1}\right) \tag{19}$$

To calculate the severity factor, it is only necessary to measure the voltage at the midpoint of the PMSM. It must be noted that, since these components (D_3 and D_5) are not contained in the EMF of the phase, components at frequencies $3/4f_s$ and $5/4f_s$, which modify the amplitude of the components, used in the diagnosis will not appear in the motor currents.

Fig. 4 shows a scheme of the proposed fault diagnosis strategy. The middle-point voltage v_1 is acquired and the fast Fourier transform (FFT) is calculated. The components at $3/4f_s$, f_s and $5/4f_s$ are extracted from the FFT and the fault severity factor is calculated according to (19).

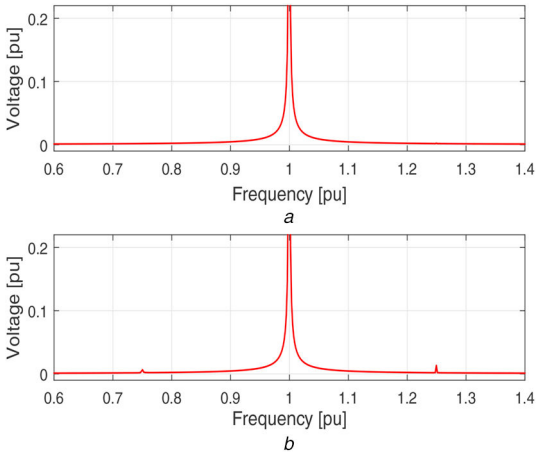

Fig. 6 *Frequency spectra of the voltages measured at*
(a) The complete phase winding, ***(b)*** Midpoint of the phase winding
Healthy PMSM

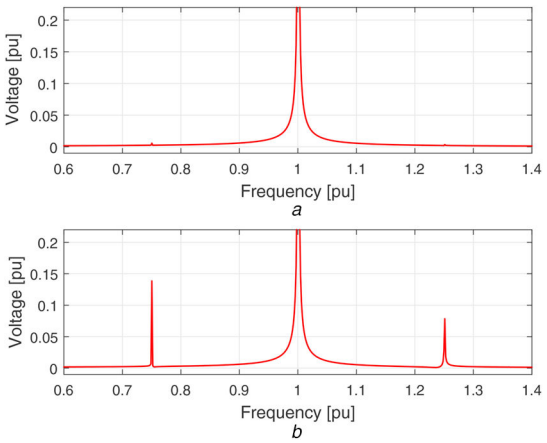

Fig. 7 *Frequency spectra of the voltages measured at*
(a) The complete phase winding, ***(b)*** Midpoint of the phase winding
PMSM with fault

3 Experimental results

To validate the proposed strategy, a PMSM with four pairs of poles was used. In this machine, the winding of a phase was modified to allow access to the midpoint. Two rotors were used for the tests (Fig. 5), one healthy and the other one from which ∼80% of one of the eight rotor magnets was removed. Voltage signals were acquired and registered with an oscillographic recorder Yokogawa OR300. For each test, 64,000 samples at 8 kHz sampling frequency were registered. The data were analysed on a personal computer.

Fig. 6 shows the frequency spectra around the fundamental component of the phase voltage and midpoint voltage of the phase, for a healthy PMSM. This figure also shows that, at frequencies $3/4f_s$ and $5/4f_s$, no components appear in the phase voltage but there are some of them of very low amplitude in the midpoint voltage. These components can be associated with the PMSM own constructive asymmetries.

Frequency spectra for the phase and the midpoint voltage for a PMSM with demagnetisation are shown in Fig. 7. As for the PMSM with no fault, it can be observed that no components appear around the fundamental component in the phase voltage spectrum. On the contrary, significant components appear on the midpoint voltage at $3/4f_s$ and $5/4f_s$ frequencies of the spectrum of the midpoint voltage of the phase.

4 Simple implementation for fault detection

This section proposes a simple implementation for the detection of faults due to demagnetisation using the voltages measured at the midpoint of the winding. Although this method does not allow for diagnosing the type of fault, it provides an indicator to trigger an

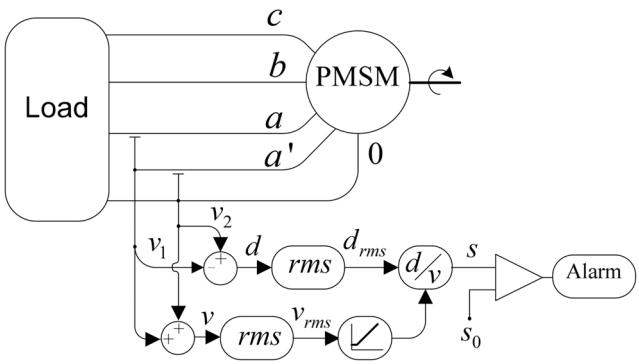

Fig. 8 *Demagnetisation detection in PMSM*

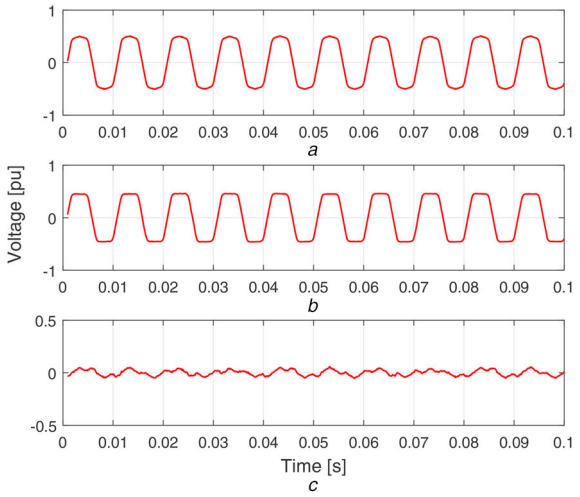

Fig. 9 *Healthy PMSM*
(a) Voltage v_1, ***(b)*** Voltage v_2, ***(c)*** Difference between v_1 and v_2

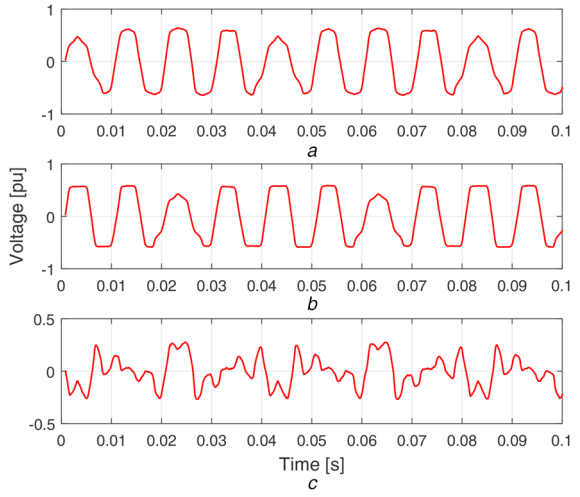

Fig. 10 *PMSM with fault*
(a) Voltage v_1, ***(b)*** Voltage v_2, ***(c)*** Difference between v_1 and v_2

alarm in the monitoring system. Fig. 8 shows a block diagram of the proposed strategy.

By subtracting the voltages of the two circuits, it can be obtained as

$$d(t) = v_1(t) - v_2(t) \tag{20}$$

Then, as the circuits are connected in series, and if in addition resistance and inductance of each circuit are equal, the voltage drops produced by them are cancelled, resulting in

$$d(t) = e_1(t) - e_2(t) \tag{21}$$

By replacing (14) and (15) in (21), it can be obtained as

$$d(t) = \sum_{\substack{n=1 \\ n \text{ odd}}}^{\infty} 2D_n \sin\left(\frac{n\omega_s}{P}t\right) \tag{22}$$

Then, the RMS value of (22) is calculated as

$$d_{\text{rms}} = \sqrt{\sum_{\substack{n=1 \\ n \text{ odd}}}^{\infty} 4D_n^2} \tag{23}$$

By replacing (9) and (17) in (23), it can be demonstrated that this RMS value is directly proportional to fault severity and the stator fundamental frequency:

$$d_{\text{rms}} \simeq \alpha\omega_s\mu \tag{24}$$

where α depends on both the winding arrangement and the distribution of the flux produced by the magnets.

For this reason, this signal can be used as an alarm to indicate demagnetisation problems in the rotor. In applications where speed does not vary significantly, it is possible to incorporate an alarm directly related to d_{rms}. However, in variable speed applications, according to (23), it will be necessary to balance the alarm system and motor speed.

Since the phase EMF of the PMSM varies linearly with speed, it can be used to normalise the signal used for fault detection. To obtain the phase EMF, it is necessary to estimate it from the phase voltages and currents of the motor. It is also necessary to know certain parameters such as phase inductances and resistances [22]. For this reason, we propose to use the phase voltage v that though it depends on the load of the PMSM, its variation from no load to full load is generally <10%. Thus the severity factor s is determined as follows:

$$s = d_{\text{rms}}/\bar{v}_{\text{rms}} \tag{25}$$

where $\bar{v}_{\text{rms}}$ is the rms value of the phase voltage limited in its minimum value to avoid division by zero. Then, this severity factor can be compared with the minimum value s_0 to trigger an alarm. Moreover, other problems such as air-gap eccentricity or stator faults may change the same indicator, so after the alarm activates, a diagnosis is required, which consists of analysing the spectrum components for the voltage at the winding midpoint.

Figs. 9 and 10 show the voltages v_1 and v_2 and the difference between a PMSM with no fault and with demagnetisation, respectively, obtained experimentally.

5 Conclusion

This work demonstrates analytically and experimentally that due to demagnetisation in the PMSM, certain components appear in the voltage spectrum of each motor winding. However, these components may not appear in the spectrum of phase voltages. Applying this novelty, a strategy for the diagnosis of this type of faults that use the voltage at the winding midpoint is proposed. A simple method to detect asymmetric demagnetisation on the windings is also presented and validated in this paper. By subtracting the voltages of the two circuits in series, the voltage drops produced by resistance and inductance of each circuit are cancelled, making the diagnosis signal less sensitive to the motor load and other disturbances that affect the phase currents. Although the midpoint of the windings is not available in many commercial motors, it is very easy to make the connection available during the manufacturing or rewinding process. This modification of the windings, although being invasive, is simpler than the placement of search coils proposed by other authors for fault diagnosis.

As further works the analysis of the effects of static and dynamic eccentricity as well as stator faults on the proposed detection strategy is proposed.

6 Acknowledgments

This work was supported in part by the Universidad Nacional de Río Cuarto, ANPCyT and the Consejo Nacional de Investigaciones Científicas y Técnicas (CONICET).

7 References

[1] Semken, R.S., Polikarpova, M., Röyttä, P., *et al.*: 'Direct-drive permanent magnet generators for high-power wind turbines: benefits and limiting factors', *IET Renew. Power Gener.*, 2012, **6**, (1), pp. 1–8

[2] Sjökvist, S., Eklund, P., Eriksson, S.: 'Determining demagnetization risk for two PM wind power generators with different PM material and identical stators', *IET Electr. Power Appl.*, 2016, **10**, (7), pp. 593–597

[3] Pellegrino, G., Vagati, A., Boazzo, B., *et al.*: 'Comparison of induction and PM synchronous motor drives for EV application including design examples', *IEEE Trans. Ind. Appl.*, 2012, **48**, (6), pp. 2322–2332

[4] Rajagopalan, S., Aller, J.M., Restrepo, J.A., *et al.*: 'Detection of rotor faults in brushless DC motors operating under nonstationary conditions', *IEEE Trans. Ind. Appl.*, 2006, **42**, (6), pp. 1464–1477

[5] Romeral, L., Urresty, J.C., Riba Ruiz, J.-R., *et al.*: 'Modeling of surface-mounted permanent magnet synchronous motors with stator winding interturn faults', *IEEE Trans. Ind. Electron.*, 2011, **58**, (5), pp. 1576–1585

[6] Urresty, J., Riba Ruiz, J.-R., Romeral, L.: 'Diagnosis of interturn faults in PMSMs operating under nonstationary conditions by applying order tracking filtering', *IEEE Trans. Power Electron.*, 2013, **28**, (1), pp. 507–515

[7] Mazzoletti, A., Bossio, G., De Angelo, C., *et al.*: 'A model-based strategy for interturn short-circuit fault diagnosis in PMSM', *IEEE Trans. Ind. Electron.*, 2017, **64**, (9), pp. 7218–7228

[8] Romeral, L., Urresty, J.C., Riba Ruiz, J.-R., *et al.*: 'Modeling of surface-mounted permanent magnet synchronous motors with stator winding interturn faults', *IEEE Trans. Ind. Electron.*, 2011, **58**, (5), pp. 1576–1585

[9] Hong, J., Lee, S.-B., Kral, C., *et al.*: 'Detection of airgap eccentricity for permanent magnet synchronous motors based on the d-axis inductance', *IEEE Trans. Power Electron.*, 2012, **27**, (5), pp. 2605–2612

[10] Ruschetti, C., Verucchi, C., Bossio, G., *et al.*: 'A model for permanent magnet synchronous machines with demagnetization faults', *IEEE Trans. Latin Am.*, 2013, **11**, (1), pp. 414–420

[11] Urresty, J., Riba Ruiz, J.-R., Delgado, M., *et al.*: 'Detection of demagnetization faults in surface-mounted permanent magnet synchronous motors by means of the zero-sequence voltage component', *IEEE Trans. Energy Convers.*, 2012, **27**, (1), pp. 42–51

[12] Urresty, J., Riba, J., Romeral, L.: 'A back-emf based method to detect magnet failures in PMSMs', *IEEE Trans. Magn.*, 2013, **49**, (1), pp. 591–598

[13] Faiz, J., Nejadi-Koti, H.: 'Demagnetization fault indexes in permanent magnet synchronous motors – an overview', *IEEE Trans. Magn.*, 2016, **52**, (4), pp. 1–11

[14] Ruschetti, C., Verucchi, C., Bossio, G., *et al.*: 'Rotor demagnetization effects on permanent magnet synchronous machines', *Energy Convers. Manage.*, 2013, **74**, pp. 1–8

[15] Choi, S., Haque, M.S., Tarek, M.T.B., *et al.*: 'Fault diagnosis techniques for permanent magnet AC machine and drives – a review of current state of the art', *IEEE Trans. Transp. Electrific.*, 2018, **4**, (2), pp. 444–463

[16] Le Roux, W., Harley, R.G., Habetler, T.G.: 'Detecting faults in rotors of PM drives', *IEEE Ind. Appl. Mag.*, 2008, **14**, pp. 23–31

[17] Faiz, J., Mazaheri-Tehrani, E.: 'Demagnetization modeling and fault diagnosing techniques in permanent magnet machines under stationary and nonstationary conditions: an overview', *IEEE Tran. Ind. Appl.*, 2017, **53**, (3), pp. 2772–2785

[18] Ruschetti, C., Bossio, G., De Angelo, C., *et al.*: 'Effects of partial rotor demagnetization on permanent magnet synchronous machines'. IEEE Int. Conf. Industrial Technology, Viña del Mar, Chile, 2010, pp. 1233–1238

[19] Casadei, D., Filippetti, F., Rossi, C., *et al.*: 'Magnets faults characterization for permanent magnet synchronous motors'. IEEE Int. Symp. on Diagnostics for Electric Machines, Power Electronics and Drives, Cargese, France, 2009, pp. 1–6

[20] Mazaheri-Tehrani, E., Faiz, J., Zafarani, M., *et al.*: 'A fast phase variable *abc* model of brushless PM motors under demagnetization faults', *IEEE Trans. Ind. Electron.*, 2019, **66**, (7), pp. 5070–5080

[21] Da, Y., Shi, X., Krishnamurthy, M.: 'A new approach to fault diagnostics for permanent magnet synchronous machines using electromagnetic signature analysis', *IEEE Trans. Power Electron.*, 2013, **28**, (8), pp. 4104–4112

[22] De Angelo, C., Bossio, G., Solsona, J., *et al.*: 'A rotor position and speed observer for permanent magnet motors with nonsinusoidal EMF waveform', *IEEE Trans. Ind. Electron.*, 2005, **52**, (3), pp. 807–813